Nanoscale

Accepted Manuscript

This article can be cited before page numbers have been issued, to do this please use: V. Urbanova, F. Karlicky, A. Matej, F. Sembera, Z. Janousek, J. A. Perman, V. Ranc, K. Cepe, J. Michl , M. Otyepka and R. Zboril, *Nanoscale*, 2016, DOI: 10.1039/C6NR00353B.

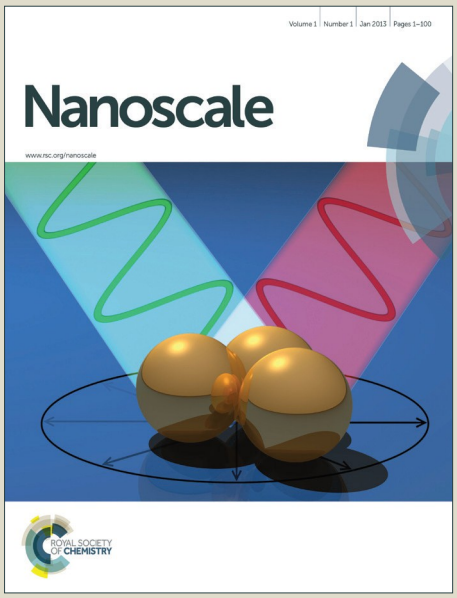

This is an *Accepted Manuscript*, which has been through the Royal Society of Chemistry peer review process and has been accepted for publication.

Accepted Manuscripts are published online shortly after acceptance, before technical editing, formatting and proof reading. Using this free service, authors can make their results available to the community, in citable form, before we publish the edited article. We will replace this *Accepted Manuscript* with the edited and formatted *Advance Article* as soon as it is available.

You can find more information about *Accepted Manuscripts* in the Information for Authors.

Please note that technical editing may introduce minor changes to the text and/or graphics, which may alter content. The journal's standard Terms & Conditions and the Ethical guidelines still apply. In no event shall the Royal Society of Chemistry be held responsible for any errors or omissions in this *Accepted Manuscript* or any consequences arising from the use of any information it contains.

ROYAL SOCIETY OF CHEMISTRY

www.rsc.org/nanoscale

View Article Online
DOI: 10.1039/C6NR00353B

Nanoscale

ARTICLE

Fluorinated graphenes as advanced biosensors - Effect of fluorine coverage on electron transfer properties and adsorption of biomolecules†

Received 27th November 2015,
Accepted 00th January 20xx

DOI: 10.1039/x0xx00000x

www.rsc.org/

Veronika Urbanová,[a] František Karlický,[a] Adam Matěj,[a] Filip Šembera,[b] Zbyněk Janoušek,[b] Jason A. Perman,[a] Václav Ranc,[a] Klára Čépe,[a] Josef Michl,[b,c] Michal Otyepka*[a] and Radek Zbořil*[a]

Graphene derivatives are promising materials for the electrochemical sensing of diverse biomolecules and development of new biosensors owing to their improved electron transfer kinetics compared to pristine graphene. Here, we report complex electrochemical behavior and electrocatalytic performance of variously fluorinated graphene derivatives prepared by reaction of graphene with a nitrogen-fluorine mixture at 2 bars pressure. The fluorine content was simply controlled by varying the reaction time and temperature. The studies revealed that electron transfer kinetics and electrocatalytic activity of CF_x strongly depend on the degree of fluorination. The versatility of fluorinated graphene as a biosensor platform was demonstrated by cyclic voltammetry for different biomolecules essential in physiological processes, i.e. NADH, ascorbic acid and dopamine. Importantly, the highest electrochemical performance, even higher than pristine graphene, was obtained for fluorinated graphene with the lowest fluorine content ($CF_{0.084}$) due to its high conductivity and enhanced adsorption properties combining π-π stacking interaction with graphene regions with hydrogen-bonding interaction with fluorine atoms.

Introduction

The discovery of graphene, *i.e.* monolayer of carbon atoms closely packed into a two-dimensional honeycomb lattice, has led to extensive research and expansion in many fields such as chemistry, biology or materials science, owing to its unique electrical, electrochemical, mechanical and optical properties.[1–7] However, pristine graphene exhibits a zero band gap, limiting its applications in nanoelectronics, photonics devices or sensors.[8] To overcome this, covalently functionalized graphene derivatives or graphene doped with various elements have been used for controlled property tailoring.[9–12] Thus, modifying graphene sheets with halogens,[13–16] hydrogen,[17–21] sulphur,[22–24] or nitrogen,[25–27] can provide new electronic, mechanical, magnetic, optical and sensing properties.[28–31]

Among the possible graphene derivatives, fluorinated graphene (CF_x) has received increased attention owing to its striking performance since fluorination is one of the most effective chemical methods to modify and control physico-chemical properties of graphene-based materials.[32–38] Fluorinated graphene has also been proposed as the ideal precursor for synthesis of new graphene derivatives through nucleophilic substitution of fluorine atoms.[39–41] Moreover, fluorinated graphenes have been reported as interesting systems creating paramagnetic centers for magnetic applications.[42,43] Importantly, the physico-chemical properties can be tuned by varying the degree of fluorination, in a way analogous to the tuning of bandgap,[44,45] dielectric[32] or electronic transfer properties.[46] However, to date, fluorinated graphenes have not been reported in sensing applications.

Fluorographene has been synthesized by various methods, such as by treatment of graphene with XeF_2,[47,48] plasma-assisted decomposition of CF_4,[49] or mechanical and chemical exfoliation of fluorographite.[47,50] In all cases, fluorine atoms are attached to the graphene scaffold via C-F covalent bonds, changing the hybrid state of carbon atoms from sp^2 to sp^3 and thereby altering the structural, optical and electronic properties of fluorographene with respect to pristine graphene.[51,52] However, control over the fluorine concentration or structure of CF_x, remains a key challenge.[46,53,54]

Fluorination of graphene may enhance the electrochemical properties and facilitate electron transfer. It seems likely that the highly electronegative fluorine bound to the graphene

[a] Regional Centre of Advanced Technologies and Materials, Department of Physical Chemistry, Faculty of Science, Palacky University in Olomouc, 17 listopadu 1192/12, 771 46 Olomouc, Czech Republic. E-mail addresses: radek.zboril@upol.cz, michal.otyepka@upol.cz
[b] Institute of Organic Chemistry and Biochemistry AS CR, v.v.i., Flemingovo nam. 2., 166 10 Prague 6, Czech Republic.
[c] Department of Chemistry and Biochemistry, University of Colorado, Boulder, Colorado 80301, United States.

†Electronic Supplementary Information (ESI) available: SEM, HRTEM, and AFM images the sheet in pristine graphene sample, Survey XPS spectrum, high resolution C 1s XPS spectrum, and Raman spectrum of pristine graphene precursor used for controlled fluorination, survey and high resolution F 1s XPS spectra of the $CF_{0.084}$, $CF_{0.158}$, and $CF_{0.218}$ samples, EDS chemical mapping of fluorine in $CF_{0.158}$, contact angle measurement of $CF_{0.084}$, $CF_{0.158}$, $CF_{0.218}$, and HOPG, and additional electrochemical data. See DOI: 10.1039/x0xx00000x

View Article Online
DOI: 10.1039/C6NR00353B

scaffold would affect the surface properties and sensing performance for various analytes and biomarkers. Faster heterogeneous electron transfer (HET) has already been shown for fluorine doped graphites,[55] and fluorinated graphene oxide[56] and was ascribed to a number of defects arising from the presence of fluorine. Additionally, fluorinated graphene can act as high performance electrode in lithium batteries[57–59] and photovoltaic cells.[60]

In this work, we report on the electrochemical performance of controllably fluorinated graphenes in sensing various physiologically important biomolecules. We identified optimal synthetic conditions enabling control of fluorine coverage whilst maintaining the dimensionality and chemical nature of the CF_x systems. Combining experimental and theoretical approaches, we found that the fluorine content had a fundamental effect on the electron transfer properties and adsorption behavior of the fluorinated graphenes. Low fluorinated graphene exhibited excellent sensing properties for all the studied biomolecules, outperforming pristine graphene, thus opening new possibilities for biosensing applications.

Experimental

Chemicals and materials

Monobasic potassium phosphate, N,N'-dimethylformamide (DMF), dibasic potassium phosphate, ß-nicotinamide adenine dinucleotide, reduced dipotassium salt (NADH), ascorbic acid and dopamine from Sigma-Aldrich were of analytical grade and used without further purification. All solutions were prepared with deionized water.

Preparation of graphene and fluorographenes with various degree of fluorination

Few layered graphene was prepared using an intense cavitation field in a pressurized ultrasonic reactor in DMF with graphite as a precursor according to a previously described method.[61] The sample was then removed from DMF using vacuum filtration and allowed to dry at 100 °C for 24 hours prior to fluorination. Three different samples of fluorinated graphene were prepared as follows: dried graphene samples (~ 25 mg) were flushed with pure N_2 gas and then treated with a nitrogen-fluorine mixture (20 vol.% F_2) in a Teflon autoclave - sample 1 was treated at 2 bars for 5 hours at room temperature , sample 2 at 2 bars for 24 hours at room temperature, and sample 3 at 2 bars for 24 hours at room temperature followed by heating to 80 °C for an additional 4 hours and left to cool to room temperature overnight.

Electrode modification

Glassy carbon electrodes (GCE, 3 mm in diameter, 2Theta Czech Republic) were polished on wet silicon carbide paper using alumina 1 and 0.05 µm Al_2O_3 powder sequentially and then washed in ethanol followed by distilled water. The GCEs were afterwards modified with fluorinated graphene samples by drop-coating: 10 µl of water dispersion (1 mg mL^{-1}) was coated onto the GCE surface and allowed to dry at room temperature.

Characterization methods

X-ray photoelectron spectroscopy (XPS) measurements were carried out with a PHI VersaProbe II (Physical Electronics) spectrometer using an Al K_α source (15 kV, 50 W). All spectra were measured in a vacuum of 1.4 x 10^{-7} Pa and at room temperature. The XPS spectra were evaluated with MultiPak (Ulvac - PHI, Inc.) software. All binding energy (BE) values were referenced to the C1s peak at 284.80 eV. Raman spectra were recorded on a DXR Raman microscope (Thermo Scientific) using the 532 nm excitation line of a diode laser. The samples were also analyzed with a scanning electron microscope (SEM) Hitachi SU6600 with an accelerating voltage 15 kV, and AFM images were obtained using a Ntegra (NT-MDT) scanning probe microscope (SPM) operating in semi-contact mode with a HaNC tip. Elemental mapping was conducted using a high resolution transmission electron microscope (HR-TEM TITAN 60-300kV) operating at 80 kV, and energy dispersive X-ray spectroscopy (EDS) with an acquisition time of 20 min was also used.

Electrochemical measurements

All electrochemical experiments were performed using a PGSTAT128N potentiostat (Metrohm Autolab B.V.) monitored by NOVA software. A conventional three-electrode cell configuration was employed. Modified GCEs were used as working electrodes, with a saturated Ag/AgCl (2Theta, Czech Republic) and a platinum wire as reference and counter electrode, respectively. All experiments were performed at room temperature.

Calculations

The projector augmented waves (PAW) method[62] as implemented in the VASP package[63] was used to perform geometry optimization using the Perdew-Burke-Ernzerhof (PBE) GGA functional[64] with empirical dispersion correction (PBE-D2).[65] An optimized graphene lattice constant of 2.468 Å was used. For fluorographene, a lattice constant of 2.607 Å, C-C distance of 1.58 Å and C-F distance of 1.38 Å were used.[66] The size of supercell was proportional to the size of simulated molecule on the surface. A 13 x 13 graphene/fluorographene supercell (containing 338 carbon atoms) was used for adsorption of the large NADH ($C_{21}O_{14}N_7P_2H_{29}$) molecule and a cut-off energy of 350 eV was applied for the plane-wave basis set during optimization together with low VASP precision. A smaller supercell of 7x7 (containing 98 carbon atoms) was used for dopamine and ascorbic acid and a cut-off energy of 400 eV and normal precision of VASP was applied. Atomic positions were relaxed until the change in energy was less than 10^{-3} eV and the first Brillouin zones were represented by gamma point. Subsequent total energy calculations were carried out using the optB86b-vdW functional,[67] which provided adsorption enthalpies of small organic molecules to graphene in excellent agreement with experimental data.[68,69] The first Brillouin zone was sampled by 2x2 k-points, the break

View Article Online
DOI: 10.1039/C6NR00353B

condition for the electronic step was an energy difference of 10^{-5} eV and a cut-off energy of 450 eV was applied together with accurate setup of VASP.

Results and discussion

Chemical composition and structural properties of fluorographenes – fluorination control

The starting graphene precursor used for controlled fluorination comprised highly transparent sheets with a thickness of a few nanometers or less as shown by AFM, SEM and HRTEM measurements (see Fig. S1 in ESI†). The pristine graphene was of high purity containing 92at% of carbon and 8at% of oxygen according to XPS data (Fig. S2 in ESI†). The small amount of oxygen is typical of graphene samples prepared by chemical exfoliation[70] and remained approximately constant in all fluorinated samples.

Survey XPS data of the fluorinated samples (Fig. S3 in ESI†) clearly showed increasing fluorine content and decreasing C/F ratio with increasing fluorination time and temperature. Namely, the sample treated for 5 hours at room temperature exhibited a C/F ratio of 11.93 (sample labelled as $CF_{0.084}$), the sample treated for 24 hours at room temperature had a lower C/F ratio of 6.31 ($CF_{0.158}$), and the sample treated for 24 hours at room temperature and then 4 hours at 80 °C showed the lowest C/F ratio of 4.59 ($CF_{0.218}$). The increasing fluorine content was also evidenced in high resolution C1s XPS spectra through increased intensities of C-F and C-F_2 bands and gradually suppressed intensities for C=C bonds, indicating decreasing content of sp^2 carbon (see Fig. 1). Similarly, Raman spectra showed an increasing I_D/I_G ratio, starting from 0.087 for the untreated graphene sample (Fig. S2 in ESI†) to 0.485 for $CF_{0.084}$, 0.503 for $CF_{0.158}$ and 0.704 for $CF_{0.218}$ with D/G bands centered at 1344/1566 cm^{-1}, 1342/1564 cm^{-1} and 1337/1566 cm^{-1}, respectively. Thus, both the XPS and Raman data unambiguously confirmed a gradually increasing content of sp^3 carbon due to the tailored fluorination procedure.

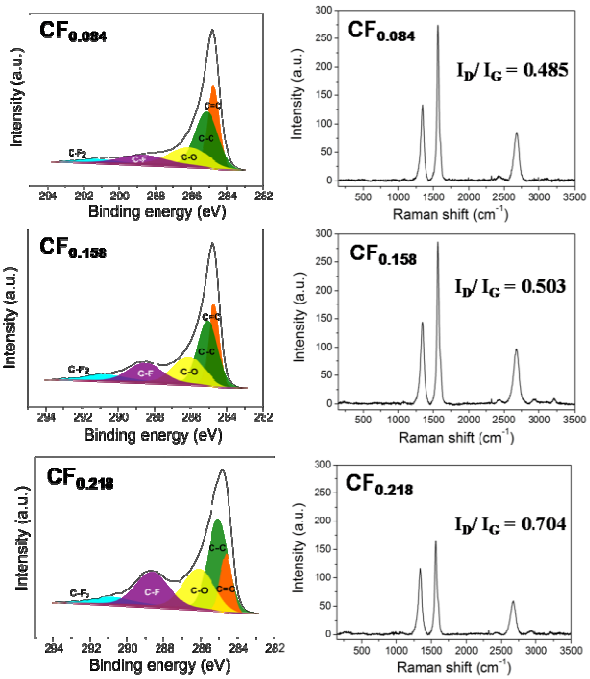

Fig. 1. High resolution C 1s XPS spectra and Raman spectra of $CF_{0.084}$ (top), $CF_{0.158}$ (middle), and $CF_{0.218}$ (bottom).

The characterization of CF_x systems was supported by HRTEM analyses and EDS chemical mapping, enabling not only the varying fluorine content but also the homogeneity/heterogeneity of its distribution over the fluorographene sheet (Fig. 2) to be monitored. Importantly, the few-layered or even single-layered character of all CF_x systems was preserved during the fluorination process, as illustrated by the highly transparent ultrathin sheets in HRTEM images (see Fig. 2, left column). EDS spectra corresponded well with XPS and Raman data, indicating increasing fluorine content with increasing reaction time and temperature. Moreover, coloured EDS chemical maps provided useful information on the fairly homogeneous distribution of fluorine over CF_x sheets, including edges (see Fig. S4 in ESI†). This finding has important implications mainly for the mechanism of electrochemical sensing.

View Article Online
DOI: 10.1039/C6NR00353B

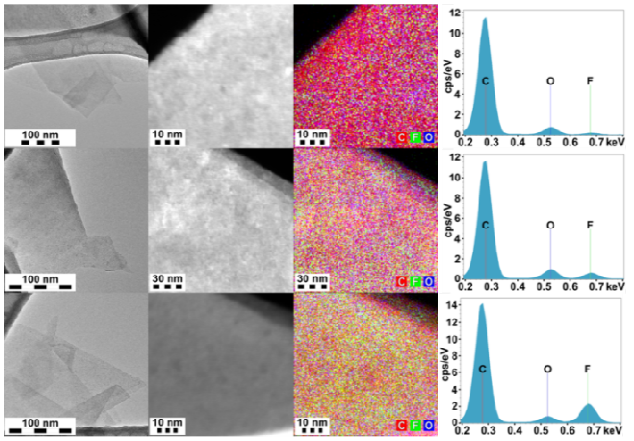

Fig. 2. HRTEM image, STEM-HAADF image, EDS elemental (C/F/O) mapping and EDS spectra of samples $CF_{0.084}$ (top), $CF_{0.158}$ (middle), and $CF_{0.218}$ (bottom).

In summary, the detailed characterization of fluorinated graphenes clearly showed that the synthetic procedure used allowed control over the fluorine content whilst maintaining the few-layered chemical character of the materials, homogeneous distribution of fluorine over the sheets and chemical nature of the fluorine atoms in CF_x systems. Indeed, the C-F and C-F_2 bands exhibited nearly the same binding energies at ~288.3 and ~290.7 eV, respectively (Fig. 1). Moreover, the high resolution F 1s XPS spectra of all fluorinated samples (Fig. S3 in ESI†) contained a peak around ~687 eV, which was uniform in shape and typical of covalently bound fluorine as similar binding energies were observed, for example, in the structure of tris(4-fluorophenyl)phosphine.[71]

Electrochemical sensing with CF_x

The electrochemical properties of CF_x modified GCEs were first investigated by cyclic voltammetry in the presence of redox probe $[Fe(CN)_6]^{4-/3-}$, as shown in Fig. 3. The peak-to-peak separation (ΔE_p) indicated faster electron transfer for the electrode modified with $CF_{0.084}$ (ΔE_p = 189 mV) compared to a bare electrode (ΔE_p = 194 mV) or electrode modified by graphene (ΔE_p = 293 mV). The electrode modified with the $CF_{0.158}$ sample offered slightly better electron transfer (ΔE_p = 246 mV) than the electrode modified by graphene, whereas the slowest electron transfer was observed for the electrode modified by fluorinated graphene with the highest fluorine content, $CF_{0.218}$ (ΔE_p = 376 mV).

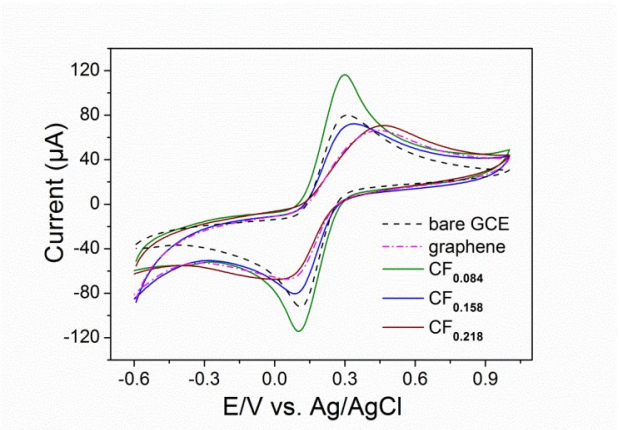

Fig. 3. (A) Cyclic voltammetry of 5 mmol L^{-1} $[Fe(CN)_6]^{4-/3-}$ recorded with glassy carbon electrodes modified with $CF_{0.084}$ (green line), $CF_{0.158}$ (blue line), $CF_{0.218}$ (brown line) and pristine graphene (dashed-dotted magenta line). The response of a bare GCE (dashed black line) is also shown. All measurements were performed in 0.1 mol L^{-1} phosphate buffer (PBS) pH 7.0 at a scan rate of 50 mV s^{-1}.

A scan rate study for sample $CF_{0.084}$ is shown in Fig. 4. A good linear relationship between the square root of the scan rate and peak current in the range of 10 mV s^{-1} to 200 mV s^{-1} with a correlation coefficient of 0.996 and 0.994 was observed (Fig. 5). This result illustrated that the electrode process is diffusion controlled.

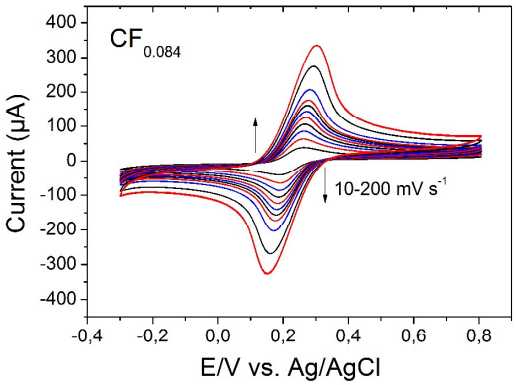

Fig. 4. Cyclic voltammograms recorded with glassy carbon electrodes modified with sample $CF_{0.084}$ at different scan rates. All measurements were performed in 0.1 mol L^{-1} phosphate buffer (PBS) pH 7.0 containing 5 mmol L^{-1} $[Fe(CN)_6]^{4-/3-}$.

View Article Online
DOI: 10.1039/C6NR00353B

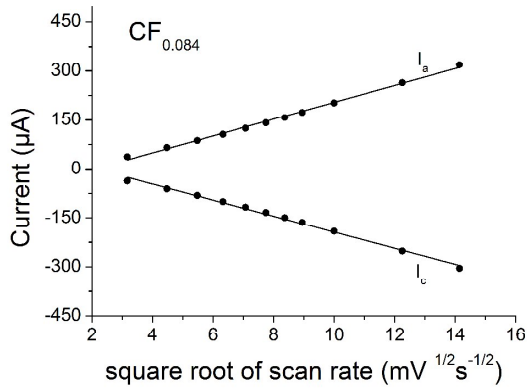

Fig. 5. Plot of anodic (I_a) and cathodic (I_c) vs. square root of scan rate.

The electron transfer properties were further characterized by electrochemical impedance spectroscopy (data not shown). The Nyquist plots were fitted by using a Randles equivalent circuit, thus taking into account diffusion and kinetic controlled parameters. The charge transfer resistance R_{ct} was represented by a semicircle in the Nyquist plot. The values of R_{ct} were in good agreement with the results obtained by cyclic voltammetry since the lowest impedance was obtained for the electrode modified with low fluorinated graphene, $CF_{0.084}$ (107 Ω), whereas the highest impedance was for the electrode modified with $CF_{0.218}$ (309 Ω) or the starting graphene (305 Ω). The electrode modified with $CF_{0.158}$ offered similar impedance to that measured for bare electrode (290 Ω). Clearly, the lowest resistance to heterogeneous electron transfer was observed for the fluorographene containing the lowest amount of fluorine on the graphene sheets. In addition, the sample with the lowest content of fluorine exhibits better hydrophilic properties compared to the other CF_x samples or pristine graphene (Fig. S5 in ESI†). It is worth noting that changes in hydrophobicity of fluorinated graphenes have already been explained in literature.[72,73] Owing to the improved hydrophilicity and high conductivity of the sample $CF_{0.084}$, one would expect improved sensing properties toward different biomolecules. To verify this hypothesis, the sensing properties of fluorinated graphenes were tested with various biomolecules, namely nicotinamide adenine dinucleotide (NADH), ascorbic acid (AA), and dopamine.

Electrochemical oxidation of NADH is of particular interest as the effective regeneration of NADH/NAD^+ system plays an essential role in many important biosynthesis reactions, in organic chemistry and as cofactors of large number of enzymes, mostly dehydrogenases,[74–75] Owing to the importance of efficient NAD^+/NADH recycling in dehydrogenase-based devices, such as biofuel cells and bioreactors, advanced NADH detection has received much attention. A key challenge in electrochemical regeneration of NAD^+ is the high overpotential required owing to slow kinetics when conventional electrodes are used.[76] Strategies to overcome this limitation include electrode modification by redox mediators such as phenothiazine or phenoxazine derivatives,[77] quinones,[78] or diaphorase enzyme,[79] More recently, different forms of carbon (e.g. pyrolitic graphite, carbon nanotubes or graphene oxide) have been utilized.[80,81] Here, for the first time, we tested the efficiency of low fluorinated graphenes. The catalytic activity of the electrodes modified by fluorinated graphenes toward NADH oxidation recorded in 0.1 mol L^{-1} phosphate buffer (pH 7.0) is shown in Fig. 6.

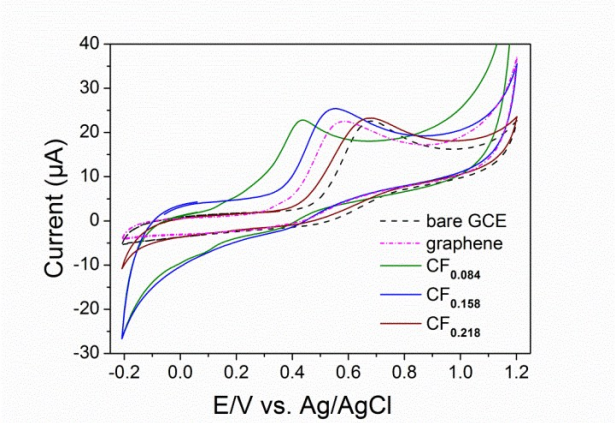

Fig. 6. Cyclic voltammograms of 2.5 mmol L^{-1} NADH at GCEs modified by fluorographene samples: $CF_{0.084}$ (green line), $CF_{0.158}$ (blue line), $CF_{0.218}$ (brown line). Responses of the GCE modified by pristine graphene (dashed-dotted magenta line) and bare GCE (dashed black line) are also shown. All measurements were performed in 0.1 mol L^{-1} phosphate buffer (PBS) pH 7.0 at a scan rate of 100 mV s^{-1}.

Well-defined oxidation peaks were observed in all cases, but after modification with $CF_{0.084}$, a remarkable potential shift of oxidation peak was achieved. The peak potential of NADH oxidation was shifted from 0.68 V on a GCE to 0.43 V after GCE modification, which could be attributed to the higher conductivity of low fluorinated $CF_{0.084}$ samples.

In order to consider the general applicability of fluorinated graphenes in biosensing, we further explored their effect toward the oxidation of two other important biomolecules, i.e., ascorbic acid (AA) and dopamine (DA). Ascorbic acid is an essential biomolecule for physiological processes in human metabolism whereas DA is a known transmitter of the nervous system and a hormone involved in many biological processes in the human brain and body. Low levels of DA are common in patients suffering from Parkinson´s disease. Abnormal DA levels are also related to schizophrenia or restless leg syndrome.[82–86]

The voltammetric responses to AA and DA for various fluorinated graphene samples are shown in Fig. 7 and 8. The lowest oxidation potential of AA was observed with a GCE modified with the low fluorinated $CF_{0.084}$ sample at 100 mV, whereas bare GCE was found to oxidize AA at 400 mV. Increasing the fluorine content in the samples resulted in a shift to the higher overpotentials and lower current response to AA (see Fig. 7), which may be ascribed to slower electron transfer.

View Article Online
DOI: 10.1039/C6NR00353B

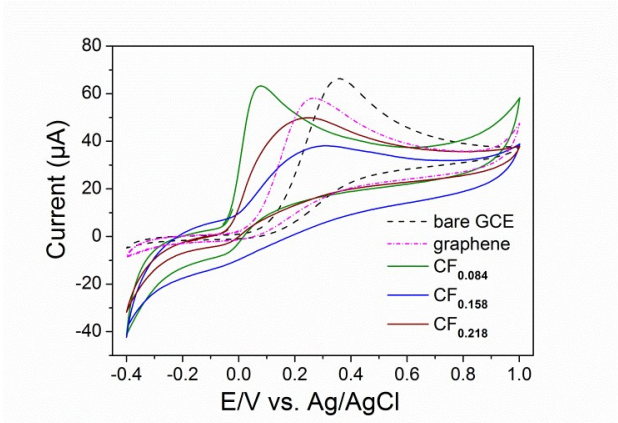

Fig. 7. Cyclic voltammetry of 5 mmol L^{-1} ascorbic acid recorded at a GCE modified by fluorographene samples: $CF_{0.084}$ (green line), $CF_{0.158}$ (blue line), $CF_{0.218}$ (brown line). Responses of a GCE modified by pristine graphene (dashed-dotted magenta line) and bare GCE (dashed black line) are also shown. All measurements were performed in 0.1 mol.L^{-1} phosphate buffer (PBS) pH 7.0 at a scan rate of 100 mV s^{-1}.

In the case of DA detection, a considerable improvement in the voltammetric response was observed when using a GCE modified with least fluorinated $CF_{0.084}$ sample (see Fig. 8). This improvement comprised not only reduction of the overpotential but also increased sensitivity towards DA compared to the other electrodes, i.e., those modified with fluorographenes with higher fluorine contents ($CF_{0.158}$ and $CF_{0.218}$), pristine graphene or bare glassy carbon.

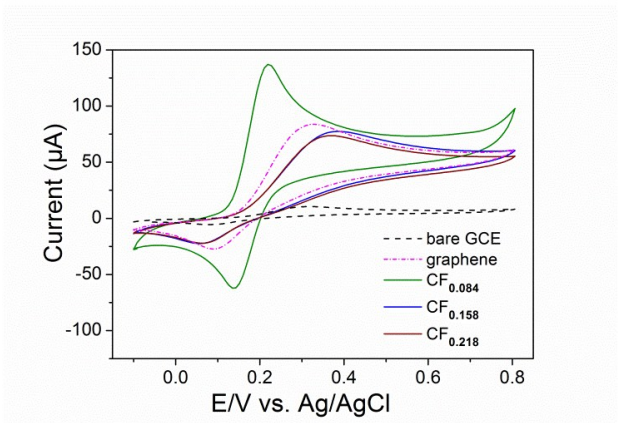

Fig. 8. Cyclic voltammetry of 5 mmol L^{-1} dopamine recorded at a GCE modified by fluorographene samples: $CF_{0.084}$ (green line), $CF_{0.158}$ (blue line), $CF_{0.218}$ (brown line). Responses of a GCE modified by pristine graphene (dashed-dotted magenta line) and bare GCE (dashed black line) are also shown. All measurements were performed in 0.1 mol.L^{-1} phosphate buffer (PBS) pH 7.0 at a scan rate of 100 mV s^{-1}.

In order to obtain closer insight about the reaction mechanism of DA oxidation at the electrode modified with $CF_{0.084}$, some additional experiments were performed (Fig. S6 in ESI†). The influence of scan rates (30 – 200 mV s^{-1}) on the electrocatalytic response of modified electrode is shown in Fig. S6A in ESI†. The peak currents increase linearly with respect to scan rate. This linear correlation revealed that the electrochemical oxidation of DA occurring on the $CF_{0.084}$ modified electrode is an adsorption controlled process[87,88] thus likely dependent on the surface properties. The concentration range was tested for modified electrode using 1 – 20 mmol L^{-1} dopamine (Fig. S6B in ESI†). The dopamine oxidation current was in this case linear up to 10 mmol L^{-1}. At the concentration above this value, the adsorption sites on the modified electrode surface become saturated. The influence of pH of supporting electrolyte on both oxidation peak current and potential are also shown (Fig. S6C,D in ESI†). The DA peak currents increased slightly with increasing pH with its maximum around pH 6.0. The potentials shifted negatively with increasing pH due to the participation of protons in the electrode reaction. The calibration plot showed good linear relationship between peak currents and the concentration of DA in the range of 0.5 – 20 μmol L^{-1} (Fig. S7 in ESI†). Linear regression is described as $I = 8.3x10^{-7}c - 1.7x10^{-7}$ with correlation coefficient 0.995. The limit of detection (LoD) for dopamine was established from the calibration curves based on the standard deviation (σ) of the response and the slope (S) that can be expressed as LoD = 3.3 x (σ/S). In this way, LoD was found to be 0.57 μmol L^{-1} and thus $CF_{0.084}$ modified electrode offering better detection limit for the determination of DA compared to previously reported sensors based on pristine graphene.[89,90]
In summary, it was shown that fluorinated graphene with very low fluorine content exhibits superior electrochemical performance and offers huge application potential for electrochemical sensing of important biomarkers as well as development of new electrochemical platforms.

Theoretical modelling of the interaction of fluorinated graphenes with biomolecules – explanation of differences in CF_x electrochemical performance

To provide an atomistic view of the observed differences in the electrochemical performance of graphenes with various degrees of fluorine coverage, we carried out DFT theoretical calculations. As the electron transfer process is the same for individual molecules, the differences may be due to different affinities between the compound and electrode material.[91,92] We calculated adsorption energies of NADH, AA, DA at typical adsorption sites on pristine graphene and variously fluorinated graphenes assuming homogeneous fluorine coverage as proved by EDS chemical mapping. We considered the following surfaces: pristine graphene, fully fluorinated graphene (C_1F_1), partially fluorinated graphene $CF_{0.25}$ (most similar to the experimental sample $CF_{0.218}$ with the highest fluorine content), and low fluorinated graphene $CF_{0.082}$ (most similar to the experimental sample $CF_{0.084}$ with the lowest fluorine content).
Table 1 shows that the adsorption of biomolecules at fully fluorinated graphene (C_1F_1) was in all cases weaker than that at pristine graphene. For the homogeneously partially fluorinated graphenes, the adsorption energy drastically increased with decreasing number of fluorine atoms. Thus, the adsorption energies of all three biomolecules to the sample with the lowest fluorine coverage ($CF_{0.082}$) were even higher than those calculated for pristine graphene.

View Article Online
DOI: 10.1039/C6NR00353B

Table 1. Adsorption energies[a] (in kcal mol^{-1}) of NADH, AA and DA on various graphene based surfaces.

Interaction surface	Adsorption energy (kcal mol^{-1}) NADH	AA	DA
Graphene	-67.6	-22.3	-21.7
Fully fluorinated graphene (C_1F_1)	-43.7	-17.5	-17.9
Partially fluorinated graphene ($CF_{0.25}$)	-38.5	-10.2	-11.0
Low fluorinated graphene ($CF_{0.082}$)	-72.9	-25.5	-26.8

[a] The optB86b-vdW density functional was used.

Concerning the mechanism behind the higher adsorption energy of biomolecules to weakly fluorinated graphene compared to pristine graphene surface, we believe that it involves a combination of π-π stacking interaction to graphene regions with hydrogen-bonding interaction to fluorine atoms (see Fig. 9). The adsorption of a molecule would therefore be most effective for low fluorinated graphene because the topology of a low concentration of fluorine atoms allows synergetic effect between the two types of bonding. Thus, we conclude that the different adsorption energies, together with different conductivities, are responsible for the differences seen in the electrochemical performance of the variously fluorinated graphenes and may explain the unusually good performance of low fluorinated graphene in sensing the tested biomolecules.

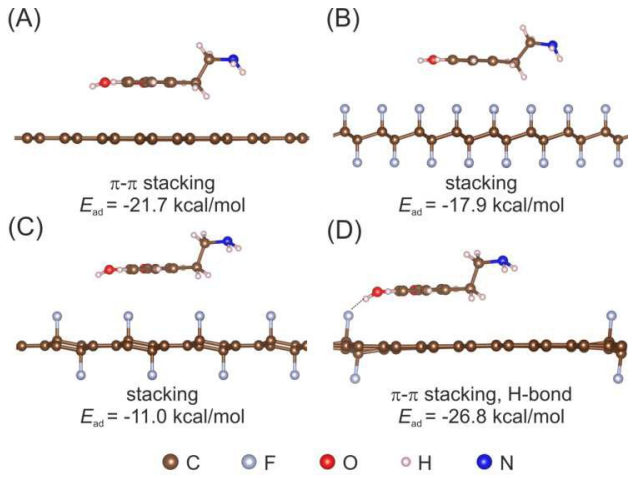

Fig. 9. Configurations of a dopamine molecule on (A) graphene, (B) fully fluorinated graphene, (C) partially fluorinated graphene $CF_{0.25}$, and (D) low fluorinated graphene $CF_{0.082}$ and corresponding adsorption energies obtained using nonlocal optB86b-vdW density functional.

Conclusions

Fluorinated graphene derivatives with controlled and homogeneous fluorine coverage were prepared by fluorination of graphene in an autoclave under increased F_2 pressure. Their electrochemical behavior and adsorption mechanism toward selected biomolecules (NADH, AA, DA) important in various physiological processes were monitored by cyclic voltammetry and DFT calculations, respectively. We found that the fluorine content had a fundamental effect on electron transfer kinetics, electrocatalytic activity and adsorption energy of the biomolecules tested. Importantly, the fluorinated graphene with the lowest fluorine content exhibited excellent sensing properties owing to its high conductivity and adsorption energy arising from π-π stacking interactions to graphene regions and hydrogen-bonding interactions to fluorine atoms. We believe this study opens the doors for application of weakly fluorinated graphenes as electrode materials for electrochemical sensing biomolecules with higher performance than the commonly used graphene/graphene oxide.

Acknowledgements

The authors gratefully acknowledge the support from the Operational Program Research and Development for Innovations - European Regional Development Fund (project LO1305 and CZ.1.07/2.3.00/30.0004 of the Ministry of Education, Youth and Sports of the Czech Republic). This work was also supported by Czech Science Foundation (Project GACR No. 15-09991S). We thank V. Štengl (Institute of Inorganic Chemistry of the Academy of Sciences of the Czech Republic) for providing us with pristine graphene precursor, J. Vlček (Palacký University) for contact angle measurements, M. Petr and K. Holá (Palacký University) for measurement and processing of XPS data, respectively. F.S. and Z.J. acknowledge support from the Institute of Organic Chemistry and Biochemistry AS CR, v.v.i. (Project no. RVO61388963).

Notes and references

1 A. K. Geim, *Science*, 2009, **324**, 1530.
2 H. Jiang, *Small*, 2011, **7**, 2413.
3 K. S. Novoselov, *Science*, 2004, **306**, 666.
4 M. Pumera, *Energy Environ. Sci.*, 2011, **4**, 668.
5 Y. Wang, Z. Li, J. Wang, J. Li and Y. Lin, *Trends Biotechnol.*, 2011, **29**, 205.
6 Y. Zhang, T. R. Nayak, H. Hong and W. Cai, *Nanoscale*, 2012, **4**, 3833.
7 H. Chang and H. Wu, *Adv. Funct. Mater.*, 2013, **23**, 1984.
8 A. H. Castro Neto, F. Guinea, N. M. R. Peres, K. S. Novoselov and A. K. Geim, *Rev. Mod. Phys.*, 2009, **81**, 109.
9 J. M. Englert, C. Dotzer, G. Yang, M. Schmid, C. Papp, J. M. Gottfried, H.-P. Steinrück, E. Spiecker, F. Hauke and A. Hirsch, *Nat. Chem.*, 2011, **3**, 279.
10 Z. Sun, D. K. James and J. M. Tour, *J. Phys. Chem. Lett.*, 2011, **2**, 2425.
11 V. Georgakilas, M. Otyepka, A. B. Bourlinos, V. Chandra, N. Kim, K. C. Kemp, P. Hobza, R. Zboril and K. S. Kim, *Chem. Rev.*, 2012, **112**, 6156.
12 L. Yan, Y. B. Zheng, F. Zhao, S. Li, X. Gao, B. Xu, P. S. Weiss and Y. Zhao, *Chem. Soc. Rev.*, 2012, **41**, 97.
13 O. Jankovský, P. Šimek, K. Klimová, D. Sedmidubský, S. Matějková, M. Pumera and Z. Sofer, *Nanoscale*, 2014, **6**, 6065.
14 F. Karlický, K. Kumara Ramanatha Datta, M. Otyepka and R. Zbořil, *ACS Nano*, 2013, **7**, 6434.

View Article Online
DOI: 10.1039/C6NR00353B

15 H. L. Poh, P. Šimek, Z. Sofer and M. Pumera, *Chem. Eur. J.*, 2013, **19**, 2655.
16 F. Karlický, R. Zbořil and M. Otyepka, *J. Chem. Phys.*, 2012, **137**, 034709.
17 Y. Li, D. Datta, Z. Li and V. B. Shenoy, *Comput. Mater. Sci.*, 2014, **83**, 212.
18 S. Ryu, M. Y. Han, J. Maultzsch, T. F. Heinz, P. Kim, M. L. Steigerwald and L. E. Brus, *Nano Lett.*, 2008, **8**, 4597.
19 A. Savchenko, *Science*, 2009, **323**, 589.
20 D. Smith, R. T. Howie, I. F. Crowe, C. L. Simionescu, C. Muryn, V. Vishnyakov, K. S. Novoselov, Y.-J. Kim, M. P. Halsall, E. Gregoryanz and J. E. Proctor, *ACS Nano*, 2015, **9**, 8279.
21 T. R. Nelson and O. V. Prezhdo, *J. Am. Chem. Soc.*, 2013, **135**, 3702.
22 W. S. V. Lee, M. Leng, M. Li, X. L. Huang and J. M. Xue, *Nano Energy*, 2015, **12**, 250.
23 H. L. Poh, P. Šimek, Z. Sofer and M. Pumera, *ACS Nano*, 2013, **7**, 5262.
24 P. A. Denis, *Chem. Phys. Lett.*, 2010, **492**, 251.
25 X. Wang, Q. Weng, X. Liu, X. Wang, D.-M. Tang, W. Tian, C. Zhang, W. Yi, D. Liu, Y. Bando and D. Golberg, *Nano Lett.*, 2014, **14**, 1164.
26 Y. Wang, Y. Shao, D. W. Matson, J. Li and Y. Lin, *ACS Nano*, 2010, **4**, 1790.
27 C. K. Chua, Z. Sofer, J. Luxa and M. Pumera, *Chem. Eur. J.*, 2015, **21**, 8090.
28 A. Criado, M. Melchionna, S. Marchesan and M. Prato, *Angew. Chem. Int. Ed.*, 2015, **54**, 10734.
29 X. Wang, Y. Liu, J. Xu, S. Li, F. Zhang, Q. Ye, X. Zhai and X. Zhao, *J. Nanomater.*, 2015, 1–14.
30 W. Wei and X. Qu, *Small*, 2012, **8**, 2138.
31 M. Wu, X. C. Zeng and P. Jena, *J. Phys. Chem. Lett.*, 2013, **4**, 2482.
32 K.-I. Ho, C.-H. Huang, J.-H. Liao, W. Zhang, L.-J. Li, C.-S. Lai and C.-Y. Su, *Sci. Rep.*, 2014, **4**, 5893.
33 I.-Y. Jeon, M. J. Ju, J. Xu, H.-J. Choi, J.-M. Seo, M.-J. Kim, I. T. Choi, H. M. Kim, J. C. Kim, J.-J. Lee, H. K. Liu, H. K. Kim, S. Dou, L. Dai and J.-B. Baek, *Adv. Funct. Mater.*, 2015, **25**, 1170.
34 P. Lazar, C. K. Chua, K. Holá, R. Zbořil, M. Otyepka and M. Pumera, *Small*, 2015, **11**, 3790.
35 N. A. Nebogatikova, I. V. Antonova, V. Y. Prinz, I. I. Kurkina, V. I. Vdovin, G. N. Aleksandrov, V. B. Timofeev, S. A. Smagulova, E. R. Zakirov and V. G. Kesler, *Phys. Chem. Chem. Phys.*, 2015, **17**, 13257.
36 A. N. Rudenko, F. J. Keil, M. I. Katsnelson and A. I. Lichtenstein, *Phys. Rev. B*, 2013, **88**, 081405.
37 P. M. Sudeep, S. Vinayasree, P. Mohanan, P. M. Ajayan, T. N. Narayanan and M. R. Anantharaman, *Appl. Phys. Lett.*, 2015, **106**, 221603.
38 Z. Sofer, P. Šimek, V. Mazánek, F. Šembera, Z. Janoušek and M. Pumera, *Chem. Commun.*, 2015, **51**, 5633.
39 M, Dubecký, E. Otyepková, P. Lazar, F. Karlický, M. Petr, K. Čépe, P. Banáš, R. Zbořil and M. Otyepka, *J. Phys. Chem. Lett.*, 2015, **6**, 1430.
40 V. Urbanová, K. Holá, A. B. Bourlinos, K. Čépe, A. Ambrosi, A. H. Loo, M. Pumera, F. Karlický, M. Otyepka and R. Zbořil, *Adv. Mater.*, 2015, **27**, 2305.
41 C. Bosch-Navarro, M. Walker, N. R. Wilson and J. P. Rourke, *J. Mater. Chem. C*, 2015, **3**, 7627.
42 R. R. Nair, M. Sepioni, I.-L. Tsai, O. Lehtinen, J. Keinonen, A. V. Krasheninnikov, T. Thomson, A. K. Geim and I. V. Grigorieva, *Nat. Phys.*, 2012, **8**, 199.
43 H. Y. Liu, Z. F. Hou, C. H. Hu, Y. Yang and Z. Z. Zhu, *J. Phys. Chem. C*, 2012, **116**, 18193.
44 Z. Wang, J. Wang, Z. Li, P. Gong, X. Liu, L. Zhang, J. Ren, H. Wang and S. Yang, *Carbon,* 2012, **50**, 5403.
45 H. Chang, J. Cheng, X. Liu, J. Gao, M. Li, J. Li, X. Tao, F. Ding and Z. Zheng, *Chem. Eur. J.*, 2011, **17**, 8896.
46 F. Withers, S. Russo, M. Dubois and M. F. Craciun, *Nanoscale Res. Lett.*, 2011, **6**, 526.
47 R. R. Nair, W. Ren, R. Jalil, I. Riaz, V. G. Kravets, L. Britnell, P. Blake, F. Schedin, A. S. Mayorov, S. Yuan, M. I. Katsnelson, H.-M. Cheng, W.; W. Strupinski, L. G. Bulusheva, A. V. Okotrub, I. V. Grigorieva, A. N. Grigorenko, K. S. Novoselov and A. K. Geim, *Small*, 2010, **6**, 2877.
48 J. T. Robinson, J. S. Burgess, C. E. Junkermeier, S. C. Badescu, T. L. Reinecke, F. K. Perkins, M. K. Zalalutdniov, J. W. Baldwin, J. C. Culbertson, P. E. Sheehan and E. S. Snow, *Nano Lett.* 2010, **10**, 3001.
49 M. Chen, H. Zhou, C. Qiu, H. Yang, F. Yu and L. Sun, *Nanotechnology*, 2012, **23**, 115706.
50 R. Zbořil, F. Karlický, A. B. Bourlinos, T. A. Steriotis, A. K. Stubos, V. Georgakilas, K. Šafářová, D. Jančík, C. Trapalis and M. Otyepka, *Small*, 2010, **6**, 2885.
51 A. L. Walter, H. Sahin, K.-J. Jeon, A. Bostwick, S. Horzum, R. Koch, F. Speck, M. Ostler, P. Nagel, M. Merz, S. Schupler, L. Moreschini, Y. J. Chang, T. Seyller, F. M. Peeters, K. Horn and E. Rotenberg, *ACS Nano*, 2014, **8**, 7801.
52 F. Karlický and M. Otyepka, *J. Chem. Theory Comput.*, 2013, **9**, 4155.
53 S. D. Sherpa, G. Levitin and D. W. Hess, *Appl. Phys. Lett.*, 2012, **101**, 111602.
54 B. Wang, J. Wang and J. Zhu, *ACS Nano*, 2014, **8**, 1862.
55 X. Chia, A. Ambrosi, M. Otyepka, R. Zbořil and M. Pumera, *Chem. Eur. J.*, 2014, **20**, 6665.
56 S. Boopathi, T. N. Narayanan and S. Senthil Kumar, *Nanoscale*, 2014, **6**, 10140.
57 D. Damien, P. M. Sudeep, T. N. Narayanan, M. R. Anantharaman, P. M. Ajayan and M. M. Shaijumon, *RSC Adv.*, 2013, **3**, 25702.
58 P. Meduri, H. Chen, J. Xiao, J. J. Martinez, T. Carlson, J.-G. Zhang and Z. D. Deng, *J. Mater. Chem. A*, 2013, **1**, 7866.
59 L. Zhan, S. Yang, Y. Wang, Y. Wang, L. Ling and X. Feng, *Adv. Mater. Interfaces*, 2014, **1**, 1300149.
60 S.-H. Kim, C.-H. Lee, J.-M. Yun, Y.-J. Noh, S.-S. Kim, S. Lee, S. M. Jo, H.-I. Joh and S.-I. Na, *Nanoscale*, 2014, **6**, 7183.
61 V. Štengl, *Chem. Eur. J.*, *2012*, **18**, 14047.
62 P. E. Blöchl, *Phys. Rev. B*, 1994, **50**, 17953.
63 G. Kresse and D. Joubert, *Phys. Rev. B*, 1999, **59**, 1758.
64 J. P. Perdew, K. Burke and M. Ernzerhof, *Phys. Rev. Lett.*, 1996, **77**, 3865.
65 S. Grimme, *J. Comput. Chem.*, 2006, **27**, 1787.
66 F. Karlický and M. Otyepka, *Ann. Phys.*, 2014, **526**, 408.
67 J. Klimeš, D. R. Bowler and A. Michaelides, *Phys. Rev. B*, 2011, **83**, 195131.
68 P. Lazar, F. Karlický, P. Jurečka, M. Kocman, E. Otyepková, K. Šafářová and M. Otyepka, *J. Am. Chem. Soc.*, 2013, **135**, 6372.
69 F. Karlický, E. Otyepková, P. Banáš, P. Lazar, M. Kocman and M. Otyepka, *J. Phys. Chem. C*, 2015, **119**, 20535.
70 N. G. Shang, P. Papakonstantinou, S. Sharma, G. Lubarsky, M. Li, D. W. McNeill, A. J. Quinn, W. Zhou and R. Blackley, *Chem. Commun.*, 2012, **48**, 1877.
71 S. Hoste, D. F. Van De Vondel and G. P. Van Der Kelen, *J. Electron Spectros. Relat. Phenomena*, 1979, **17**, 191.
72 V. Mazanek, O. Jankovsky, J. Luxa, D. Sedmidubsky, Z. Janousek, F. Sembera, M. Mikulics, Z. Sofer, *Nanoscale*, 2015, **7**, 13646.
73 P. Wang, H. Wang, W. Yang, *Phys. Chem. Chem. Phys.,* 2014*,* **16**, 20464.
74 L. Gorton, P. N. Bartlett, In *Bioelectrochemistry: Fundamentals, Experimental techniques and Applications*; Ed.; Wiley: Chichester, England, UK; 2008; pp 157–198.
75 H. K. Chenault and G. M. Whitesides, *Appl. Biochem. Biotechnol.*, 1987, **14**, 147.

View Article Online
DOI: 10.1039/C6NR00353B

76 H. Zhao and W. A. van der Donk, *Curr. Opin. Biotechnol.*, 2003, **14**, 583.
77 H. Li, R. Li, R. M. Worden and S. C. Barton, *ACS Appl. Mater. Interfaces*, 2014, **6**, 6687.
78 R. A. Rincón, K. Artyushkova, M. Mojica, M. N. Germain, S. D. Minteer and P. Atanassov, *Electroanalysis*, 2010, **22**, 799.
79 D. Dicu, F.-D. Munteanu, I. Catalin Popescu and L. Gorton, *Anal. Lett.*, 2003, **36**, 1755.
80 B. Limoges, D. Marchal, F. Mavré and J.-M. Savéant, *J. Am. Chem. Soc.*, 2006, **128**, 2084.
81 S. P. Kumar, R. Manjunatha, C. Nethravathi, G. S. Suresh, M. Rajamathi and T. V. Venkatesha, *Electroanalysis*, 2011, **23**, 842.
82 C. S. Lim, C. K. Chua and M. Pumera, *Analyst*, 2014, **139**, 1072.
83 P. Damier, *Brain*, 1999, **122**, 1437.
84 R. D. O'Neill, *Sensors*, 1995, **5**, 317.
85 G. S. Wilson and M. A. Johnson, *Chem. Rev.*, 2008, **108**, 2462.
86 V. Ranc, Z. Markova, M. Hajduch, R. Prucek, L. Kvitek, J. Kaslik,K. Safarova and R. Zboril, *Anal. Chem.*, 2014, **86**, 2939.
87 A. G. Zestos, Ch. Yang, C. B. Jacobs, D. Hensley and B. J. Venton, *Analyst*, 2015, **140**, 7283.
88 E. Laviron, *J. Electroanal. Chem. Interfacial Electrochem.*, 1979, **101**, 19.
89 Y. R. Kim, S. Bong, Y. J. Kang, Y. Yang, R. K. Mahajan, J. S. Kim, H. Kim, *Biosens. Bioelectron.*, 2010, **25**, 2366.
90 S. Qi, B. Zhao, H. Tang, X. Jiang, *Electrochim. Acta*, 2015, **161**, 395.
91 M. Pumera, R. Scipioni, H. Iwai, T. Ohno, Y. Miyahara and M. Boero, *Chem. Eur. J.*, 2009, **15**, 10851.
92 K. H. Hui, M. Pumera and A. Bonanni, *Chem. Eur. J.*, 2015, **21**, 11793.

TOC